Optimisation of Petroleum Production Well Placement under Geological Uncertainty

PROCEEDINGS OF THE 30th European Symposium on Computer Aided Process Engineering (ESCAPE30), May 24-27, 2020, Milano, Italy

Optimisation of petroleum production well placement under geological uncertainty

Emmanuel I. Epelle, Dimitrios I. Gerogiorgis

Institute for Materials and Processes (IMP), School of Engineering, University of Edinburgh, The Kings Buildings, Edinburgh, EH9 3FB, United Kingdom
D.Gerogiorgis@ed.ac.uk

Abstract

Large investments are required for the positioning and drilling of oil and gas wells, implying that decisions related to these activities may be significantly aided by sound and proven mathematical-oriented methods. The use of intuitive engineering judgement alone cannot guarantee sustainable profitability over long periods, especially under geological (reservoir model) uncertainty. To capture significant uncertainty sources in the subsurface geology of the reservoir considered in this study, geostatistical model realisations are obtained using available information (permeabilities and porosities). We use specialised algorithms of the MATLAB Reservoir Simulation Toolbox (MRST, interfaced with PETREL™) in order to determine optimal petroleum production well locations and production rates and thus maximise the field oil recovery. The developed computational workflow has been applied to a realistic case study, for which robust optimality is demonstrated using the worst-case realisation for determining optimal well locations.

Keywords: Production optimisation; optimal well placement; geological uncertainty.

1. Introduction

Well placement optimisation at the early planning stages of field development is necessary to achieve the best possible economic benefits. Reservoir simulations that quantify fluid flow behaviour with respect to well positions can be used to describe subsurface flow phenomena over a long time horizon. However, these simulations can be computationally expensive and this limits the number of iterations that can be performed in the search for an optimal operation strategy. The application of mathematical optimisation to well placement problems usually includes gradient-based methods, mixed integer programming, genetic algorithms and particle swarm optimisation (Bangerth et al., 2006; Onwunalu and Durlofsky, 2010). The complexity of this problem is aggravated by geological uncertainty, which can be accounted for by incorporating multiple geological realisations in the optimisation formulation. The use of the entire superset and a subset of equiprobable geological realisations for well placement optimisation has been carried out by Yeten et al. (2003) and Wang et al. (2012), with intense computational efforts. However, the application of flow diagnostics adopted in this work for well placement optimisation, utilises an adjoint code for gradient evaluations (Møyner et al., 2015), thus enabling faster and accurate computations compared to previous studies. The objective of the present study is to offer a systematic exploration of different operational strategies (with flow visualisations) for optimal oil recovery, demonstrated on a realistic field using the functionalities of the MATLAB Reservoir Simulation Toolbox (MRST).

2. Methodology

Static modelling: The first step in this stage involves the mapping of horizons and faults from the available seismic data in PETREL™ (Figs. 1a and 1b). This is followed by the creation of surface maps that mark the reservoir's boundary (Fig. 1c). Well log interpretations are carried out next to identify the productive geological zones based on the reservoir's lithology, porosity and fluid resistivity (Fig. 1d). The result of this interpretation is the final static model as shown in Fig. 1e, which is upscaled for dynamic simulation purposes (Fig. 1f). The field contains 5 injection wells and 3 production wells.

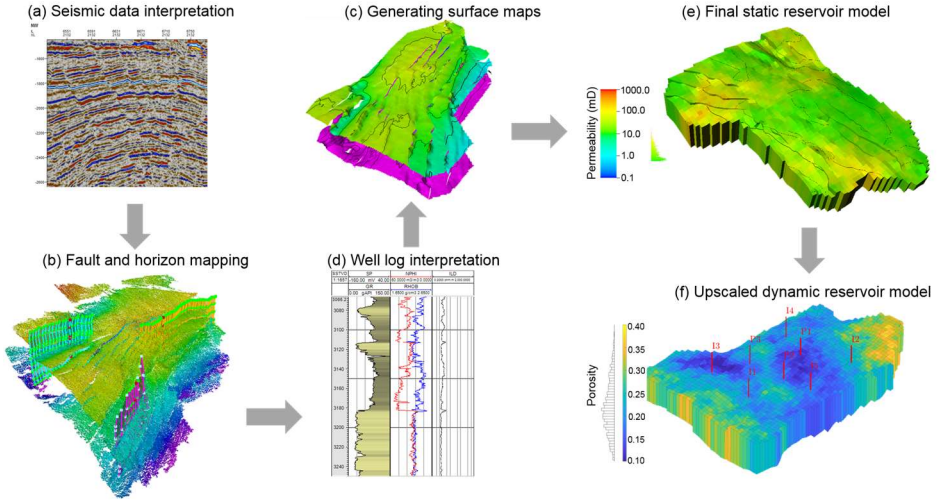

Figure 1: Static and dynamic reservoir model development procedure.

Incorporating uncertainty: Geological uncertainty exists because it is difficult to know the exact properties of every section of the realistic reservoir (Rahim and Li, 2015). Using the sequential Gaussian simulation functionality of PETREL™, 50 realisations of the reservoir's permeability (horizontal and vertical) are generated. The grid structure and the fluid and rock properties of each realisation are imported into MATLAB (where optimisation tasks are performed using the MRST toolbox). The Lorenz coefficient (L_c) is the main ranking metric applied and the worst realisation is that with the highest L_c.

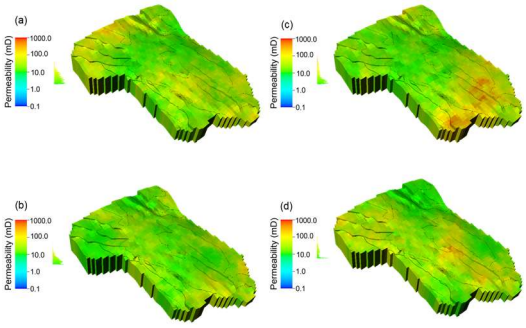

Figure 2: 4 out of 50 geological realisations.

Dynamic modelling and optimisation formulation: Optimisation tasks are carried out over the worst case scenario after ranking the geological realisations, thus ensuring robust feasibility of the obtained solution (worst-case optimisation). The mathematical formulation of the reservoir model, objective function, operational constraints and adopted solution strategy (Møyner et al., 2015) are shown in Table 1. The dynamic reservoir model (Eqs. 1–3) describes the flow field in the reservoir and the time-of-flight (TOF, the time required for a fluid particle to travel along a streamline from its starting

point to the current position). The pressure is denoted as p, the TOF as τ, the Darcy velocity as $\vec{v}$, the reservoir's storage capacity as ϕ, the permeability tensor as $\mathbf{K}$, and the fluid mobility as λ_f. Flow in the reservoir can be driven by wells, n_{bh}, which are controlled by the bottomhole pressure (BHP), but also by other wells, n_r, which are rate controlled. Both well types, n_w, have perforations, n_{pf}, through which fluid flows from the reservoir into the wellbore. All wells are modelled using the Peaceman well model (Eq. 4) in which the well perforation fluxes are denoted by q_{pf}. The index of the well to which perforation number j belongs is denoted as $N_w(j)$. Moreover, k is the well index and W^j_{pf} is the Peaceman well index. Furthermore, a set of manipulations (controls), in the form of closure relations, are specified for each well type (Eqs. 5–6); $\mathbf{u}$ is the control vector.

Table 1: Modelling and optimisation framework for well placement optimisation.

Reservoir Model

$$\mathcal{P}(q,\vec{v}) = \nabla \times \vec{v} - q = 0 \quad (1)$$

$$\mathcal{V}(p,\vec{v}) = \vec{v} + \mathbf{K}\lambda_f \nabla p = 0 \quad (2)$$

$$\mathcal{T}(\tau,\vec{v}) = \vec{v} \times \nabla\tau - \phi = 0 \quad (3)$$

$$\mathcal{Q}^j(q_{pf}, q_{pf}, p) = q^j_{pf} - W^j_{pf}\lambda_f\left[p^{N_w(j)}_{bh} - p\right] = 0; j = 1, \dots, n_{pf} \quad (4)$$

$$\mathcal{C}_{bh} = u^k_{bh} - p^k_{bh} = 0; k = 1, \dots, n_{bh} \quad (5)$$

$$\mathcal{C}_r = u^k_r - \sum_{j \in N_{pf}(k)} q^j_{pf} = 0; k = n_{bh}+1, \dots, n_{bh} \quad (6)$$

Objective Function & Constraints

$$L_{c,o} = 2\int_0^1 [F(\phi) - \phi]\, S_o d\phi \quad (7)$$

$$NPV(T) = \int_{t=0}^{T} \sum_{c=o,w} (r_c q_c + r_{ci} q_{ci})\,(1+d)^{-1} dt \quad (8)$$

$$u \leftarrow u - P\left(\alpha \frac{dG_\lambda}{d\boldsymbol{u}}\right)^T \quad (9)$$

Solution Strategy

$$\begin{bmatrix} 0 & \partial_v\mathcal{P} & \partial_q\mathcal{P} & 0 \\ \partial_p\mathcal{V} & \partial_v\mathcal{V} & 0 & 0 \\ \partial_p\mathcal{Q} & 0 & \partial_q\mathcal{Q} & \partial_{p_{bh}}\mathcal{Q} \\ 0 & 0 & \partial_q\mathcal{C} & \partial_{p_{bh}}\mathcal{C} \end{bmatrix} \begin{bmatrix} \mathbf{p} \\ \mathbf{v} \\ \mathbf{q} \\ \mathbf{p_{bh}} \end{bmatrix} = \begin{bmatrix} 0 \\ 0 \\ 0 \\ 0 \end{bmatrix} \quad (10)$$

Adjoint Formulation

$$G_\lambda = G[\boldsymbol{x}(\boldsymbol{u}), \boldsymbol{u}] + \lambda^T g[\boldsymbol{x}(\boldsymbol{u}), \boldsymbol{u}] \quad (11)$$

$$\frac{dG_\lambda}{d\boldsymbol{u}} = \frac{\partial G}{\partial \boldsymbol{u}} + \left(\frac{\partial G}{\partial \boldsymbol{x}} + \lambda^T \frac{\partial g}{\partial \boldsymbol{x}}\right)\frac{\partial x}{\partial \boldsymbol{u}} + \lambda^T \frac{\partial g}{\partial \boldsymbol{u}} + \boldsymbol{g}^T \frac{\partial \lambda}{\partial \boldsymbol{u}} \quad (12)$$

$$\left(\frac{\partial g}{\partial \boldsymbol{x}}\right)^T \lambda = \mathbf{J}^T\lambda = -\left(\frac{\partial G}{\partial \boldsymbol{x}}\right)^T \quad (13)$$

$$\frac{dG_\lambda}{d\boldsymbol{u}} = \frac{\partial G}{\partial \boldsymbol{u}} + \lambda^T \frac{\partial g}{\partial \boldsymbol{u}} \quad (14)$$

Besides the well placement optimisation, rate control optimisation is subsequently performed on the optimally located wells. The first objective function (Eq. 7) is applied to the well placement optimisation task; the objective function is based on the Lorenz coefficient (Eq. 7), which is written in terms of the flow capacity, F, and the storage capacity, ϕ. This coefficient measures how the oil displacement efficiency for a given well pattern differs from that of an ideal (piston-like) displacement pattern in the reservoir. Thus, this coefficient is a measure of the optimality of the water flooding operation and hence the oil recovery in the reservoir. However, a simplified Net Present Value (NPV) expression (without installation cost of wells and other factors) is utilised as the objective function of the rate control procedure (Eq. 8). T represents the length of the time horizon, q_c and q_{ci} are the field production and injection rates of components c (oil and water) respectively. The revenues and costs of production and injection of components c are r_c and r_{ci} respectively and d is the discount rate. Furthermore, we note that $\boldsymbol{\mathcal{C}}$, $\boldsymbol{\mathcal{T}}$, $\boldsymbol{\mathcal{V}}$, $\boldsymbol{\mathcal{Q}}$ and $\boldsymbol{\mathcal{P}}$ represent the discretised system in terms of variables, q_{pf}, p_{bh}, p, v, τ.

To perform optimisation computations, the primary variables (pressure, rates and TOF) in Eqs. 1–3 are solved for, and the objective function gradients are computed for a set of controls. The solution strategy (two-point flux approximation for spatial discretisation – Eq. 10) minimises computational workload and makes it adaptable to different linear

algebraic solvers. The adjoint equations comprises the Lagrange function for the problem (Eq. 11), its derivatives (Eq. 12) and simplifications (Eqs. 13–14) that yield an objective function which depends on the state variables, **x** and not on the control variables **u**. $\mathbf{x}^T$ is a vector of the solution quantities $\mathbf{p}^T$, $\mathbf{v}^T$, τ^T, $\mathbf{q}^T$ and $\mathbf{p}_{bh}{}^T$. G[**x**(**u**)] represents the objective function and **g**[**x**(**u**),**u**] = 0 represents a set a constraints; λ is the Lagrange multiplier, **J** is the Jacobian, and superscript *T* denotes the vector/matrix transpose, as applicable above.

Optimal well controls: A steepest-descent algorithm is implemented for finding optimal controls (Eq. 9). This utilises the supplied *NPV* objective function, the well rate bounds (maximum and minimum) and voidage replacement; α represents the step size and *P* is a projection to the constraints. While evaluating the objective, the value of α is adjusted and the algorithm stops when the improvement in the objective function between two successive iterations is less than the specified tolerance (in this case, equal to: 5×10^{-4}).

Well placement algorithm: The algorithm begins by adding pseudowells with a zero-rate in the region around each injector and computes the gradients of the added wells (based on the Lorenz coefficient). The original well is then replaced by the pseudowell with the largest gradient. The process is repeated until all wells remain stationary.

3. Simulation and optimisation results

In carrying out the optimisation procedure it is assumed that the production wells have been drilled whereas the injection wells are yet to be drilled. Thus, the aim of the optimisation task to determine the optimal injection well positions that yields the best possible oil displacement in the reservoir. In our case study, the reservoir model contains 2,726 cells with an initial pressure of 500 bar; two phases are present (oil and water). Densities and viscosities of both phases are 859 kg m^{-3}, 1014 kg m^{-3}, 2 cP and 0.5 cP respectively; the relative permeability exponents of both phases were set as 2. All 5 injection wells and 3 production wells are assumed to have vertical geometries. The initial injector placement was done such as to maintain good hydraulic connectivity between the injection and production wells given the faulted nature of the reservoir – this is based on reservoir engineering judgement (Fig. 3a). However, on applying the well placement algorithm, optimal injector locations that guarantee improved oil sweep are obtained. This can be observed in the oil saturation plots for both placement patterns (unexplored regions of the reservoir - the yellow patches in Fig. 3a are absent in Fig. 3b). The well paths taken by the algorithm during the search for optimal injector well position are shown in Fig. 3c.

The Lorenz coefficient (a measure of reservoir heterogeneity and the efficiency of oil displacement) is also shown for the two placement scenarios. A smaller value of this parameter represents a better displacement scenario; this is the case with the optimised well positions as shown in Fig. 3b compared to Fig. 3a. F/ϕ denotes the ratio of the reservoir's flow capacity to its storage capacity (Fig. 4a). For a perfect/idealised oil displacement in the reservoir, the F/ϕ ratio = 1. It is observed that the optimised well placement yields an F/ϕ curve closer to an idealised displacement scenario compared to initial well positions. In order to further validate the optimality of the new well configurations determined by the algorithm, we run multiphase flow simulations for a production timeframe of 5 years and obtain the oil recovery over this period. It is shown in Fig. 4b that the oil recovery of the optimised well placement far supersedes that of the initial well placement (twice the recovery of the initial placement at the end of the production forecast – Fig. 4b). This indicates that intuitive-based well placements will hardly yield similar performance and oil recovery (field profitability) to that obtained by

sound mathematical techniques. The well placement algorithm thus capitalises on the underlying permeability distribution for optimal determination of injection well locations.

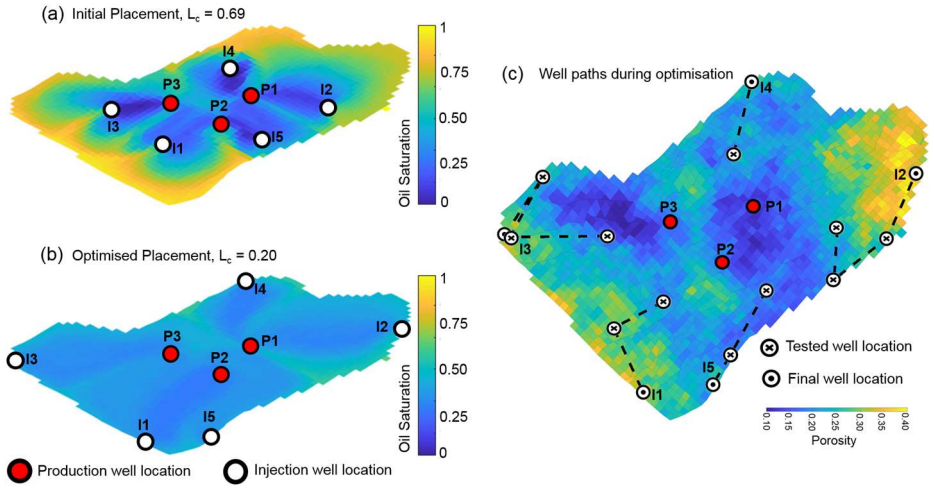

Figure 3: Oil saturation distribution before and after well placement optimisation.

The optimal control configurations (injection and production rates for respective wells) based on the new well placements are thus illustrated in Fig. 4c and 4d, respectively.

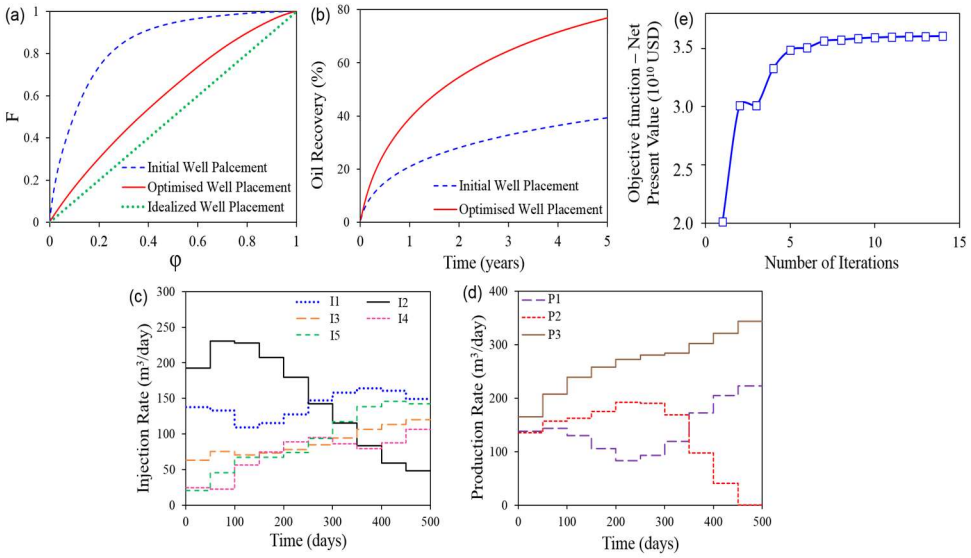

Figure 4: (a) Oil displacement efficiency F/ϕ diagram, (b) percentage oil recovery, optimal manipulations for injection (c) and production (d) wells in the field considered, (e) NPV evolution.

The application of the rate optimisation algorithm, which is based on the *NPV* indicates that injection well I2 with a steady decreasing injection rate at each timestep should be allocated the highest injection rate at the start of production. Next in magnitude is I1 with a relatively lower injection rate. I4 has the lowest injection rate compared to other injection wells and may be considered the least performing. Since operators have control over the injection rates at the surface, it can be said that the rate optimisation algorithm also inherently solves a rate allocation problem. The production rate responses from the

different wells indicates that P3 is the most productive well and significantly contributes to the overall field *NPV*. The evolution of the *NPV* objective function is shown in Fig. 4e. It is observed that within the first 5 iterations, the algorithm is able to find a near optimal solution. Compared to a methodology that requires numerous direct calls to a high-fidelity simulator or an approximation of the simulator's output (Epelle and Gerogiorgis, 2019a; b), the implemented algorithm attains optimality in fewer iterations (within 2 min of run time). Although the presented case study is somewhat small (in terms of the number of wells), such rapid computational performance is also expected when the problem size increases. Beyond the computational time required for the rate control optimisation step, we present the time required for the entire workflow (Fig. 5). Most of the time is spent on static model development and preliminary dynamic simulations to ascertain performance.

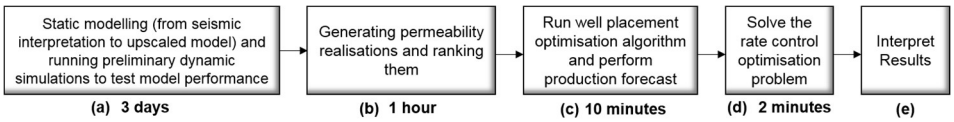

Figure 5: Time requirement for each step of the computational workflow.

4. Conclusion

This study presents an injection well placement and rate control problem of a realistic oil field under geological uncertainty. A worst-case scenario optimisation is performed based on 50 geological realisations obtained from static reservoir modelling, via Sequential Gaussian Simulation. By implementing a well placement optimisation algorithm, oil recovery in the field is boosted to twice the value obtained via intuition-based methods (for a 5-year forecast period). Furthermore, the robust computational methodology for rapid determination of gradients enables rate control (using *NPV* is the objective function) and well placement optimisation (using the Lorenz coefficient as the objective function). These tasks are performed in a matter of minutes, thus demonstrating the applicability of the implemented approach towards real-time decision support in reservoir management.

5. References

W. Bangerth, H. Klie, M.F. Wheeler, P.L. Stoffa and M.K. Sen, 2006. On optimization algorithms for the reservoir oil well placement problem. *Comput. Geosci.*, 10, 3, 303–319.

E.I. Epelle and D.I. Gerogiorgis, 2019a. A multiperiod optimisation approach to enhance oil field productivity during secondary petroleum production. *Comput. Aided Chem. Eng.,* 46, 1651–1656.

E.I. Epelle and D.I. Gerogiorgis, 2019b. Optimal rate allocation for production and injection wells in an oil and gas field for enhanced profitability. *AIChE J.*, 65, 6 (DOI: 10.1002/aic.16592).

O. Møyner, S. Krogstad and K.A. Lie, 2015. The application of flow diagnostics for reservoir management. *SPE J.*, *20*(02), 306–323.

J.E. Onwunalu and L.J. Durlofsky, 2010. Application of a particle swarm optimization algorithm for determining optimum well location and type. *Comput. Geosci.*, 14, 1, 183–198.

S. Rahim and Z. Li, 2015. Reservoir geological uncertainty reduction: an optimization-based method using multiple static measures. *Math. Geosci.*, 47, 4, 373–396.

H. Wang, D. Echeverría-Ciaurri, L.J. Durlofsky and A. Cominelli, 2012. Optimal well placement under uncertainty using a retrospective optimization framework. *SPE J.*, 17, 1, 112–121.

B. Yeten, L.J. Durlofsky and K. Aziz, 2003. Optimization of nonconventional well type, location, and trajectory. *SPE J.*, 8, 3, 200–210.